NONLINEAR CONVECTION IN MUSHY LAYERS

M. Grae Worster[1], D.M. Anderson[2] & T.P Schulze[1]

[1]Institute of Theoretical Geophysics, Department of Applied Mathematics and Theoretical Physics, Silver Street, Cambridge CB3 9EW, ENGLAND.

[2]Applied and Computational Mathematics Division, National Institute of Standards and Technology, Gaithersburg, MD 20899, USA.

INTRODUCTION

When alloys solidify in a gravitational field there are complex interactions between solidification and natural, buoyancy-driven convection that can alter the composition and impair the structure of the solid product. The particular focus of this project has been the compositional convection within mushy layers that occurs in situations where the lighter component of the alloy is rejected into the melt during solidification by cooling from below. The linear stability of such a situation was described at the 2nd Microgravity Fluid Physics Conference [1] and has been further elucidated in a number of published articles [2–4]. Here we describe some recent developments in the study of the nonlinear evolution of convection in mushy layers.

The system under consideration is illustrated in figure 1. A two-component alloy is solidified upwards at a constant rate V. It is completely solid at temperatures below the eutectic temperature T_E in the region $z < 0$, where z is the vertical coordinate in a frame of reference moving with the solidification rate. Between the eutectic front ($z = 0$) and the liquidus isotherm (at $z = h(x, y, t)$), solid and liquid coexist in close proximity within a mushy layer. At temperatures above the liquidus temperature the alloy is completely molten. The mush–liquid interface is a free boundary whose position $z = h(x, y, t)$ has to be calculated. We have studied convecting states that are steady in the moving frame of reference and have analyzed the stability of those states.

The dimensionless governing equations in the mushy layer are

$$\left(\frac{\partial}{\partial t} - \frac{\partial}{\partial z}\right)(\theta - S\phi) + \mathbf{u}\cdot\nabla\theta = 0, \tag{1}$$

$$\left(\frac{\partial}{\partial t} - \frac{\partial}{\partial z}\right)[(1-\phi)\theta + C\phi] + \mathbf{u}\cdot\nabla\theta = 0, \tag{2}$$

$$\mathbf{u} = -\Pi(\phi)(\nabla p + R_m\theta\hat{\mathbf{z}}), \tag{3}$$

$$\nabla\cdot\mathbf{u} = 0, \tag{4}$$

where

$$\theta = \frac{T - T_L(C_0)}{\Delta T} = \frac{C - C_0}{\Delta C}, \tag{6}$$

$\Delta T = T_L(C_0) - T_E$, $\Delta C = C_0 - C_E$, represents both the dimensionless temperature and the dimensionless liquid composition, since they are coupled by the liquidus relationship $T = T_L(C)$ throughout the mushy layer. The mushy layer is treated as a porous medium with locally isotropic permeability $\Pi(\phi)$ that is a function of the local solid fraction ϕ. Convection in the system is

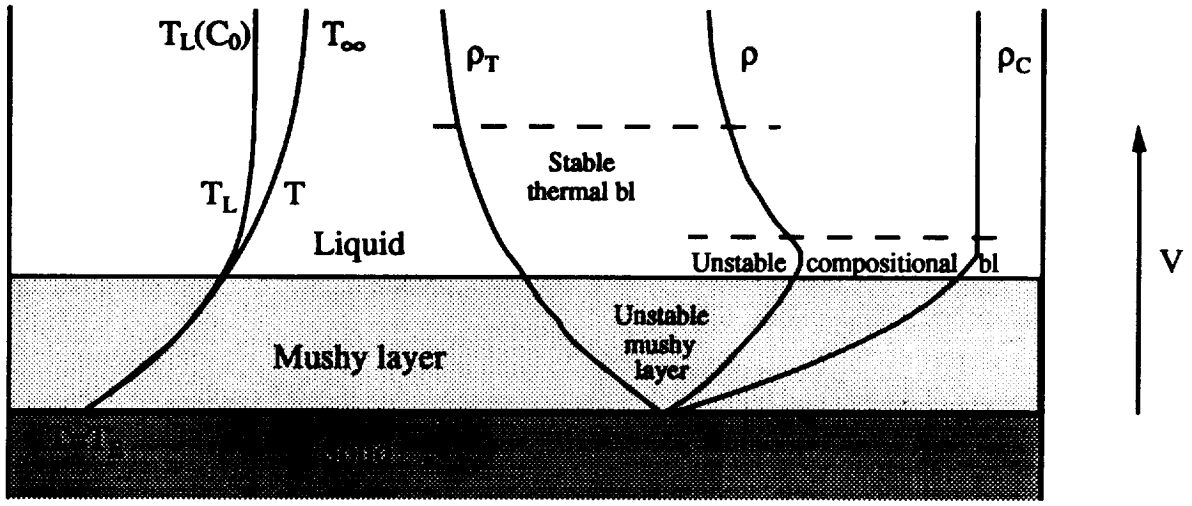

Figure 1. A schematic diagram showing the steady upwards solidification of an alloy at speed V. On the left is shown the steady temperature profile T and the profile of liquidus temperature $T_L(C)$, which is proportional to the local concentration of the liquid C, in the absence of flow. These give rise to the density profiles shown on the right. The overall density $\rho = \rho_T + \rho_C$ is unstably stratified throughout the mushy layer and can give rise to convection in the mushy layer leading to the formation of chimneys.

controlled by the Rayleigh number

$$R_m = \frac{\beta \Delta C g \Pi^*}{\nu V} \tag{7}$$

mediated by the dimensionless parameters

$$S = \frac{L}{C_p \Delta T}, \qquad \mathcal{C} = \frac{C_s - C_0}{C_0 - C_E} \qquad \text{and} \qquad \theta_\infty = \frac{T_\infty - T_L(C_0)}{\Delta T}. \tag{8,9,10}$$

Interactions between the liquid and mushy regions are further influenced by the Darcy number

$$\mathcal{H} = \frac{\kappa^2 / V^2}{\Pi^*}, \tag{11}$$

which is proportional to the square of the ratio of macroscopic lengthscales to the interstitial lengthscale of the mushy layer and is typically very large. One effect of this is that the dynamic boundary condition at the mush–liquid interface is simply that the pressure is continuous.

WEAKLY NONLINEAR ANALYSIS

We have determined the evolution of small, finite-amplitude perturbations to the steady state with no fluid flow. The coupled equations in the mushy and liquid regions are extremely complex so we have analysed a simpler system in which the mush–liquid interface is assumed to be horizontal, fixed in the moving frame and impermeable to fluid flow. This greatly simplifies the analysis without compromising the modelling of processes that are internal to the mushy layer. The fixed dimensionless height of the mushy layer δ replaces θ_∞ as a controlling parameter. In the basic, steady state of the full system, $\delta = 1/\theta_\infty$.

The dependent variables are expanded in the form

$$\theta = \theta_B(z) + \epsilon \hat{\theta}(x, y, z, t) \tag{12}$$

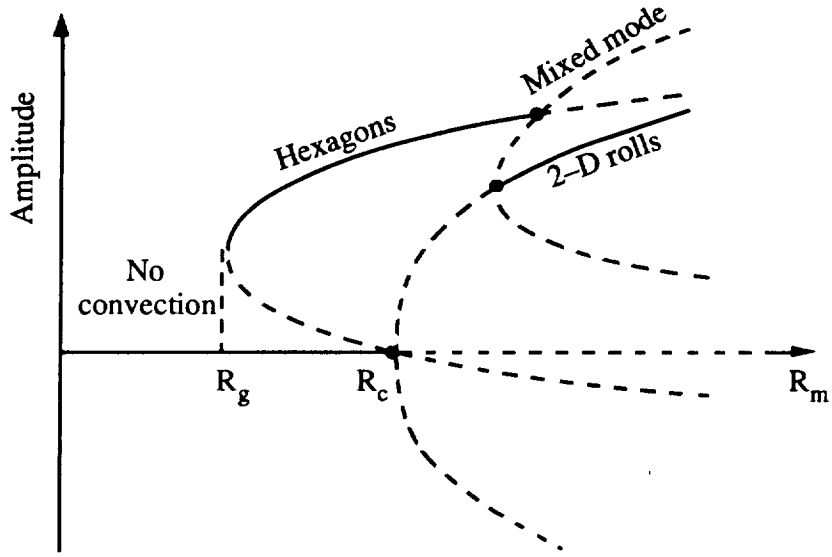

Figure 2. The nonlinear bifurcation diagram determined from the small-amplitude expansions. Solid curves indicate stable steady states of the system, while dashed curves indicate unstable steady states. In the parameter regime investigated, convection with a hexagonal planform bifurcates sub-critically while convection in the form of two-dimensional rolls bifurcates super-critically. The analysis has determined the global stability limit R_g and its explicit dependence on the various dimensionless parameters of the system. When the Rayleigh number $R_m < R_g$ no convection can occur in the mushy layer.

(with similar expressions for ϕ and $\mathbf{u}$), where $\epsilon \ll 1$ measures the perturbation amplitude. To simplify the analysis further we employed the near-eutectic approximation [5], which amounts to taking the distinguished asymptotic limit $\delta \ll 1$, with $\mathcal{C} = O(\delta^{-1})$ and $S = O(\delta^{-1})$. To leading order in this limit one recovers the analysis of convection in a passive porous medium [6]. Phenomena intrinsic to a mushy layer are then reintroduced at $O(\delta)$.

The central result of this analysis is a set of coupled evolution equations

$$a\dot{A}_1 = 2\pi R_2 A_1 + bA_2 A_3^* - cA_1|A_1|^2 - dA_1(|A_2|^2 + |A_3|^2), \tag{13}$$

$$a\dot{A}_2 = 2\pi R_2 A_2 + bA_1 A_3^* - cA_2|A_2|^2 - dA_2(|A_1|^2 + |A_3|^2), \tag{14}$$

$$a\dot{A}_3 = 2\pi R_2 A_3 + bA_2 A_1^* - cA_3|A_3|^2 - dA_3(|A_2|^2 + |A_1|^2), \tag{15}$$

for the amplitudes of three intersecting two-dimensional rolls oriented at 120° to each other. Using these equations one can determine steady two-dimensional convection by setting two of the amplitudes to zero, or steady convection with hexagonal planform by setting the three amplitudes to be equal. Such steady states were analysed by Amberg & Homsy [7]. The fully coupled equations allow interactions between these modes of convection and their stability to be determined. The structure of the nonlinear bifurcation diagram in the vicinity of the linear critical point $R_m = R_c$ is illustrated in figure 2.

The figure is drawn for the case $b > 0$ in which the first stable steady convecting state has hexagonal planform with upflow in the centres of the hexagons. This is the case when the nonlinear interactions are dominated by the variation in the permeability with solid fraction [7], which has long been thought to be the primary interaction leading to focusing of the flow. However, experiments [8] have indicated that convection in mushy layers is initiated in the form of hexagons with downflow at their centres. Our analysis [9] has shown that b can have either sign, i.e. that hexagons

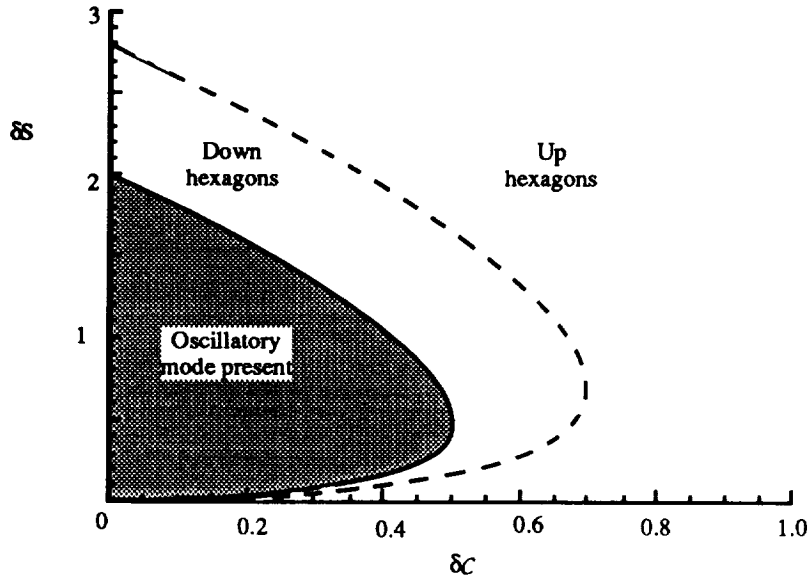

Figure 3. A diagram showing the regions of parameter space where convection in the form of either up-flowing or down-flowing hexagons are the preferred stable mode. The shaded region shows the parameter values where oscillatory convection is predicted to occur.

with either upflow or downflow at their centres can be the preferred, stable mode, depending on the dimensionless parameters of the system, as indicated in figure 3.

OSCILLATORY CONVECTION

A surprising result of the nonlinear analysis is the fact that the coefficient of the time derivative, a, can be negative for certain parameter values. This signals the existence of a hitherto unsuspected oscillatory mode of convection. A detailed linear analysis [10] has revealed such an oscillatory instability, in which the convection can take the form of travelling rolls. Although these might be difficult to observe directly, they leave a signature in the solid in the form of slanted regions of compositional alteration. Perhaps more importantly, the discovery of the oscillatory mode has highlighted a significant interaction between convection and solidification within mushy layers that has previously been neglected in asymptotic analyses.

THE FORMATION OF CHIMNEYS

The small-amplitude perturbation analysis shows that the solid fraction becomes zero inside the mushy layer when the upward velocity becomes sufficiently large. It suggests the formation of narrow, vertical channels of zero solid fraction — chimneys. Chimneys have been observed in many laboratory experiments, particularly those in which ammonium chloride is crystallized from solution [11–13] and those in which metallic alloys are solidified from below [14].

An important question is, following the nonlinear bifurcation from the linear critical point, does a chimney form first on the lower, unstable branch or on the upper, stable branch. In the latter case, finite-amplitude, steady convection can exist without the formation of chimneys. In the

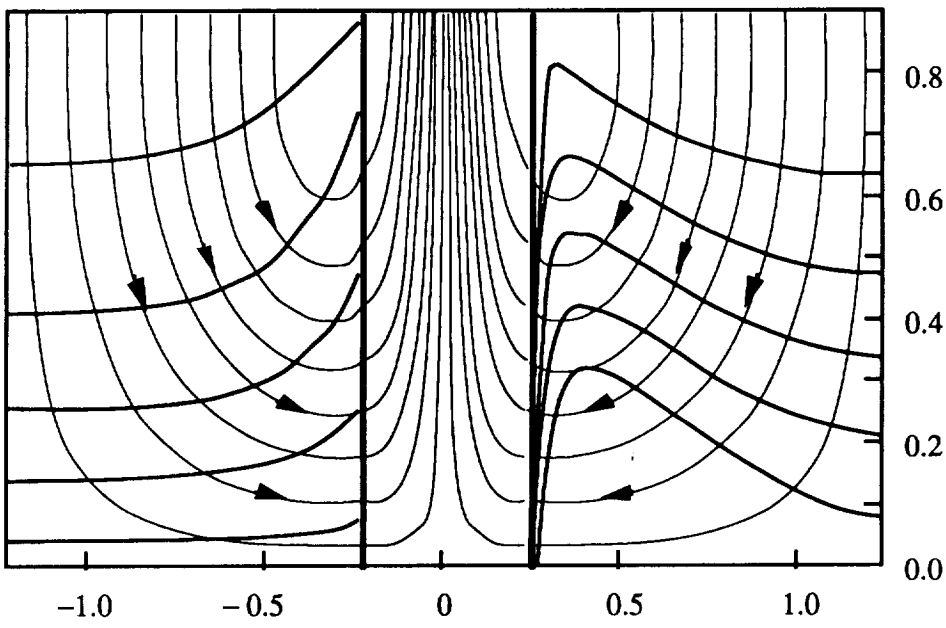

Figure 4. The thin lines show the streamlines through the mushy layer and up through a chimney (the central portion). Superposed on the left, in thicker curves, are isotherms. Superposed on the right are contours of solid fraction. The width of the chimney and the aspect ratio of the mushy layer are not to scale. The width of the chimney is inversely proportional to the cube root of the Darcy number $\mathcal{H}$ and so is typically much narrower than its height.

former case, any triggering of convection must lead inexorably to the formation of chimneys. The weakly nonlinear analysis reveals that either can occur depending on the dimensionless parameters of the system. Our recent numerical study of the fully nonlinear system has confirmed this finding.

FULLY DEVELOPED CHIMNEYS

In many systems, chimneys may be difficult to avoid. It then becomes important to be able to assess their effect on the structure of and compositional variations within a casting. To this end, models have been proposed for convection through fully developed chimneys. Roberts & Loper [15] developed a framework for such a model in which each chimney is treated as a vertical cylinder of possibly varying radius in which the liquid flows in response to its own buoyancy and the pressure at the chimney wall. The wall pressure and the heat and mass fluxes through the chimney wall couple to the flow and heat transfer in the rest of the mushy layer. This idea was adopted by Worster [16], who presented a scaling analysis, valid for $R_m \gg 1$, that revealed the structure of the flow and the temperature distribution in the mushy layer. We have recently used this same idea in a numerical evaluation of steady convecting states in a mushy layer with fully developed chimneys. The calculations performed to date have been two-dimensional. The flow in the chimney is solved using an approximate analysis based on lubrication theory. This analysis provides dynamic boundary conditions for the flow, temperature distribution and solid fraction in the mushy lyaer, which are calculated numerically.

Typical results are shown in figure 4. The depth of the mushy layer was allowed to vary dynamically, controlled in an average way by the heat transfer from the overlying liquid region.

However, the mush–liquid interface was kept horizontal. Nevertheless, the contours of solid fraction are strongly indicative that the mush–liquid interface should be raised to form a conical vent around the chimney, as has been observed in experiments. It is also apparent from figure 4 that the solid fraction at first increases towards the chimney before decreasing sharply to zero very close to the wall.

From calculations such as these we shall be able to extend the weakly nonlinear bifurcation diagram (figure 2) into strongly nonlinear regimes. From a practical point of view, we are able to calculate the solute fluxes from the mushy layer to the liquid region and hence to calculate macrosegregation in castings. Further, we plan to investigate the stability of such fully convecting states in order to determine the mean spacing between chimneys.

CONCLUSIONS

Studies of nonlinear convection in mushy layers have elucidated the parametric controls on the plan form of convection and the global stability limit for convection leading to chimney formation. Depending on parameter values, finite-amplitude convection can exist in a mushy layer without chimneys forming or the onset of convection can lead inexorably to the formation of chimneys. Numerical analyses of convection in mushy layers with fully developed chimneys have revealed the internal structure of a convecting mushy layer and promise to yield important results concerning macrosegregation in cast alloys.

REFERENCES

1. Worster, M.G. (1994) *Proc. 2nd Microgravity Fluid Physics Conf. NASA Conference Publication 3276* 193–198.
2. Worster, M.G. (1992). *J. Fluid Mech.* **237** 649–669.
3. Emms, P. & Fowler, A.C. (1994) *J. Fluid Mech.* **262**, 111–139.
4. Chen, F., Lu, J.W. & Yang, T.L. (1994) *J. Fluid Mech.* **276**, 163–187.
5. Fowler, A.C. (1985) *IMA J. Appl. Maths* **35**, 159–174.
6. Palm, E., Weber, J.E. & Kvernvold, O. (1972) *J. Fluid Mech.* **54**, 153–161.
7. Amberg, G. & Homsy, G.M. (1993) *J. Fluid Mech.* **252**, 79–98.
8. Tait, S., Jahrling & Jaupart, C. (1992) *Nature* **359**, 406–408.
9. Anderson, D. & Worster, M.G. (1995) *J. Fluid Mech.* **302**, 307–331.
10. Anderson, D. & Worster, M.G. (1996) *J. Fluid Mech.* **307**, 245–267.
11. Copley, S.M., Giamei, A.F., Johnson, S.M. & Hornbecker, M.F. (1970) *Metall. Trans.* **1**, 2193–2204.
12. Chen, F. & Chen, C.F. (1991) *J. Fluid Mech.* **227**, 567–586.
13. Tait, S. & Jaupart, C. (1992) *J. Geophys. Res.* **97**(B5), 6735–6756.
14. Sample, A.K. & Hellawell, A. (1984) *Metallurgical Transactions A* **15A**, 2163–2173.
15. Roberts, P. & Loper, D.E. (1983) In *Stellar and Planetary Magnetism*, ed. AM Soward 329-349.
16. Worster, M.G. (1991) *J. Fluid Mech.* **224**, 335–359.